Dipeptide Nanotubes, with N-Terminally Located ω-Amino Acid Residues, That are Stable Proteolytically, Thermally, and Over a Wide Range of pH

Samit Guha,[†,‡] Michael G. B. Drew,[§] and Arindam Banerjee*[,†,‡]

Chemistry Division, Indian Institute of Chemical Biology, Jadavpur, Kolkata 700 032, India, Department of Biological Chemistry, Indian Association for the Cultivation of Science, Jadavpur, Kolkata 700 032, India, and School of Chemistry, The University of Reading, Whiteknights, Reading RG6 6AD, United Kingdom

Received November 5, 2007

Two dipeptides containing an N-terminally positioned ω-amino acid residue (β-alanine/δ-amino valeric acid) self-assembles to form nanotubes in the solid state as well as in aqueous solution. In spite of having hollow nanotubular structures in the solid state and in solution, their self-assembling nature in these two states are different and this leads to the formation of different internal diameters of these nanotubes in solution and in solid state structure. These nanotubes are stable proteolytically, thermally, and over a wide range of pH values (1−13). The role of water molecules in nanotube formation has been investigated in the solid state. These nanotubes can be considered as a new class of dipeptide nanotubes as they are consisting of N-terminally located protease resistant ω-amino acid residues and C-terminally positioned α-amino acid residues. These dipeptides can form an interesting class of short peptidic structure that can give rise to stable nanotubular structure upon self-assembly and these nanotubes can be explored in future for potential nanotechnological applications.

Introduction

Design and construction of nanomaterials from self-assembly of small organic molecules using the "bottom-up" approach is a rapidly expanding area of current research.[1] In recent years, considerable attention has been directed toward the rational design of peptide-based nanotubular structures, as they can be used as glucose transporters, transmembrane ion channels, and as potential antibiotics against drug-resistant bacteria and in other fields of bionanotechnology.[2] Ghadiri and co-workers have pioneered the field of constructing cyclic oligopeptide based nanotubes in which oligopeptide rings with alternating D- and L-α-amino acid residues are stacked one on top of the other through intermolecular hydrogen bonds to form nanotubular structures.[3] Granja and co-workers have demonstrated that self-assembling peptide nanotube based on a hybrid of α-γ-cyclic peptides and it holds considerable promise for the design of nanotubes with novel structural properties.[4] Another class of peptide nanotubes reported in the literature is based on acyclic dipeptides. Linear hydrophobic water-soluble dipeptides based exclusively on α-amino acids such as Ala, Val, Ile, Leu, and Phe can form nanotubes, and in these cases, the peptide chains are interconnected mainly through head-to-tail ($NH_3^+ \cdots {}^-OOC$) hydrogen bonds.[5] The formation of nanotubes using the self-assembly of the Phe−Phe dipeptide is of particular interest as this sequence is the core recognition element in the β-amyloid polypeptide that forms the amyloid fibrils responsible for Alzheimer's disease and these nanotubes are used as templates to produce silver nanowires.[1a,6] Terminally protected short acyclic peptide based nanotubes belong to another type of peptide nanotube.[7] Water can play a key role in forming and stabilizing various supramolecular

* E-mail: arindam@iicb.res.in or arindam.bolpur@yahoo.co.in. Fax: 91-33-2473-5197.
† Indian Institute of Chemical Biology.
‡ Indian Association for the Cultivation of Science.
§ The University of Reading.

(1) (a) Reches, M.; Gazit, E. *Science* **2003**, *300*, 625–627. (b) Reches, M.; Gazit, E. *Nano Lett.* **2004**, *4*, 581–585. (c) Song, Y.; Challa, S. R.; Medforth, C. J.; Qiu, Y.; Watt, R. K.; Peña, D.; Miller, J. E.; van Swol, F.; Shelnutt, J. A. *Chem. Commun.* **2004**, 1044–1045. (d) Gupta, M.; Bagaria, A.; Mishra, A.; Mathur, P.; Basu, A.; Ramakumar, S.; Chauhan, V. S. *Adv. Mater.* **2007**, *19*, 858–861. (e) Yan, X.; He, Q.; Wang, K.; Duan, L.; Cui, Y.; Li, J. *Angew. Chem., Int. Ed.* **2007**, *46*, 2431–2434. (f) Zhang, X.; Zhang, X.; Zou, K.; Lee, C. S.; Lee, S. T. *J. Am. Chem. Soc.* **2007**, *129*, 3527–3532. (g) Zhang, X.; Zhang, X.; Shi, W.; Meng, X.; Lee, C. S.; Lee, S. T. *Angew. Chem., Int. Ed.* **2007**, *46*, 1525–1528.

(2) (a) Granja, J. R.; Ghadiri, M. R. *J. Am. Chem. Soc.* **1994**, *116*, 10785–10786. (b) Ranganathan, D. *Acc. Chem. Res.* **2001**, *34*, 919–930. (c) Quesada, J. S.; Isler, M. P.; Ghadiri, M. R. *J. Am. Chem. Soc.* **2002**, *124*, 10004–10005. (d) Fernandez-Lopez, S.; Kim, H. S.; Choi, E. C.; Delgado, M.; Granja, J. R.; Khasanov, A.; Kraehenbuehl, K.; Long, G.; Weinberger, D. A.; Wilcoxen, K. M.; Ghadiri, M. R. *Nature* **2001**, *412*, 452–455. (e) Gao, X.; Matsui, H. *Adv. Mater.* **2005**, *17*, 2037–2050.

(3) (a) Bong, D. T.; Clark, T. D.; Granja, J. R.; Ghadiri, M. R. *Angew. Chem., Int. Ed.* **2001**, *40*, 988–1011. (b) Hartgerink, J. D.; Granja, J. R.; Milligan, R. A.; Ghadiri, M. R. *J. Am. Chem. Soc.* **1996**, *118*, 43–50.

(4) (a) Brea, R. J.; Amorin, M.; Castedo, L.; Granja, J. R. *Angew. Chem., Int. Ed.* **2005**, *44*, 5710–5713. (b) Amorin, M.; Castedo, L.; Granja, J. R. *J. Am. Chem. Soc.* **2003**, *125*, 2844–2845.

(5) (a) Görbitz, C. H. *Acta Crystallogr., Sect. C* **2006**, *62*, o328–o330. (b) Görbitz, C. H. *New J. Chem.* **2003**, *27*, 1789–1793. (c) Görbitz, C. H. *Chem.−Eur. J.* **2001**, *7*, 5153–5159. (d) Görbitz, C. H. *Acta Crystallogr., Sect. B* **2002**, *58*, 849–854. (e) Görbitz, C. H. *Acta Crystallogr., Sect. E* **2004**, *60*, o626–o628.

(6) (a) Abramovich, L. A.; Reches, M.; Sedman, V. L.; Allen, S.; Tendler, S. J. B.; Gazit, E. *Langmuir* **2006**, *22*, 1313–1320. (b) Reches, M.; Gazit, E. *Curr. Nanosci.* **2006**, *2*, 105–111. (c) Görbitz, C. H. *Chem. Commun.* **2006**, 2332–2334.

(7) (a) Crisma, M.; Toniolo, C.; Royo, S.; Jiménez, A. I.; Cativiela, C. *Org. Lett.* **2006**, *8*, 6091–6094. (b) Ray, S.; Haldar, D.; Drew, M. G. B.; Banerjee, A. *Org. Lett.* **2004**, *6*, 4463–4465.

10.1021/cm703159b CCC: $40.75
Published on Web 02/28/2008

architectures through hydrogen bonding.[8] Gorbitz's L-Leu−L-Leu, L-Leu−L-Phe, L-Phe−L-Leu, and L-Ile−L-Leu dipeptide molecules, which form a nanotubular structure, contain water molecules in the core channel.[5c–e] Tryptophylglycine monohydrate is another example of a dipeptide that forms an extended, one-dimensional, water-filled nanotubular structure, which exhibits negative thermal expansion.[9] However, it is challenging to construct robust peptide-based nanotubes that can exhibit stability against various environmental responses such as heat, wide range of pH, and enzymatic degradation.[1a,d,3b,6a] In this report, we present the formation of thermally stable synthetic dipeptide nanotubes (DPNTs) in the solid state as well as in solution. These nanotubes are also stable over a broad range of pH. The role of water molecules in the nanotube formation in the solid state has also been investigated. Our reported DPNTs are somewhat different from previously reported DPNTs[1a,5] chemically and structurally, as water molecules play a vital role in the formation and stabilization of hydrogen-bonded water-mediated nanotubular structure in the solid state and this type of pattern has never been observed for regular dipeptide nanotubes. In addition, these dipeptide molecules contain ω-amino acid residues [β-alanine (β-Ala)/δ-amino valeric acid (δ-Ava)] in the N-terminal position instead of the previously reported α-amino acid residues, and these residues are found to enhance the proteolytic stability against enzymatic degradation.

Experimental Section

General Methods and Materials. β-alanine and δ-amino valeric acid were purchased from Sigma chemicals. HOBt (1-hydroxybenzotriazole) and DCC (dicyclohexylcarbodiimide) were purchased from SRL.

Peptide Synthesis. All the peptides (**1** and **2**) were synthesized by conventional solution-phase methods using racemization free fragment condensation strategy. The Boc group was used for N-terminal protection and the C-terminus was protected as a methyl ester. Couplings were mediated by dicyclohexylcarbodiimide/1-hydroxybenzotriazole (DCC/HOBt). Methyl ester deprotection was performed via the saponification method, and the Boc group was deprotected by 98% formic acid. All the intermediates were characterized by 300 MHz ^{1}H NMR and mass spectrometry. The final compounds were fully characterized by 600 MHz ^{1}H NMR spectroscopy, 300 MHz ^{1}H NMR spectroscopy, ^{13}C NMR spectroscopy, DEPT 135, mass spectrometry, and IR spectroscopy.

(a) Boc-β-Ala-OH. A solution of β-alanine (2.67 g, 30 mmol) in a mixture of dioxane (60 mL), water (30 mL), and 1 N NaOH (30 mL) was stirred and cooled in an ice–water bath. Ditert-butylpyrocarbonate (7.2 g, 33 mmol) was added, and stirring was continued at room temperature for 6 h. The solution was then concentrated in a vacuum to about 20−30 mL, cooled in an ice–water bath, covered with a layer of ethyl acetate (about 50 mL), and acidified with a dilute solution of $KHSO_4$ to pH 2–3 (Congo red). The aqueous phase was extracted with ethyl acetate, and this operation was done repeatedly. The ethyl acetate extracts were pooled, washed with water, and dried over anhydrous Na_2SO_4, and evaporated in a vacuum. A white crystalline material was obtained.

Yield: 5.35 g (28.3 mmol, 94%).

Anal. Calcd for $C_8H_{15}NO_4$ (189): C, 50.78; H, 7.99; N, 7.40.

Found: C, 50.81; H, 7.97; N, 7.43.

(b) Boc-δ-Ava-OH. A solution of δ-amino valeric acid (3.51 g, 30 mmol) in a mixture of dioxane (60 mL), water (30 mL), and 1 N NaOH (30 mL) was stirred and cooled in an ice–water bath. Ditert-butylpyrocarbonate (7.2 g, 33 mmol) was added, and stirring was continued at room temperature for 6 h. Then the solution was concentrated in a vacuum to about 20−30 mL, cooled in an ice–water bath, covered with a layer of ethyl acetate (about 50 mL) and acidified with a dilute solution of $KHSO_4$ to pH 2–3 (Congo red). The aqueous phase was extracted with ethyl acetate, and this operation was done repeatedly. The ethyl acetate extracts were pooled, washed with water, dried over anhydrous Na_2SO_4, and evaporated in a vacuum. The pure material was obtained.

Yield: 5.95 g (27.4 mmol, 91%).

Anal. Calcd for $C_{10}H_{19}NO_4$ (217): C, 55.28; H, 8.81; N, 6.45.

Found: C, 55.32; H, 8.85; N 6.42.

(c) Boc-β-Ala(1)-Ala(2)-OMe. 3.78 g (20 mmol) of Boc-β-Ala-OH was dissolved in 10 mL of DMF in an ice–water bath. H-Ala-OMe was isolated from 5.58 g (40 mmol) of the corresponding methyl ester hydrochloride by neutralization, subsequent extraction with ethyl acetate, and ethyl acetate extract was concentrated to 10 mL. It was then added to the reaction mixture, followed immediately by 4.12 g (20 mmol) of dicyclohexylcarbodiimide (DCC) and 2.7 g (20 mmol) of HOBt. The reaction mixture was allowed to come to room temperature and stirred for 3 days. The residue was taken up in ethyl acetate (40 mL) and dicyclohexylurea (DCU) was filtered off. The organic layer was washed with 1 N HCl (3 × 30 mL), brine (1 × 30 mL), 1 M sodium carbonate (3 × 30 mL), and brine (2 × 30 mL); dried over anhydrous sodium sulfate; and evaporated in a vacuum. A white material was obtained.

Yield: 4.77 g (17.4 mmol, 87%).

^{1}H NMR (300 MHz, $CDCl_3$): δ 6.22 (br, 1H, Ala(2) NH); 5.16 (br, 1H, β-Ala(1) NH); 4.53−4.63 (m, 1H, Ala(2) C^α H); 3.76 (s, 3H, -OCH_3); 3.41−3.42 (m, 2H, β-Ala(1) C^β Hs); 2.44 (t, J = 6 Hz, 2H, β-Ala(1) C^α Hs); 1.43 (s, 9H, Boc CH_3); 1.40 (d, J = 7 Hz, 3H, Ala(2) C^β Hs).

HRMS m/z 297.0966 $[M + Na]^+$, 313.0536 $[M + K]^+$; M_{calcd} = 274.3126.

Anal. Calcd for $C_{12}H_{22}N_2O_5$ (274): C, 52.54; H, 8.08; N, 10.21.

Found: C, 52.51; H, 8.11; N, 10.19.

(d) Boc-δ-Ava(1)-Phe(2)-OMe. 4.34 g (20 mmol) of Boc-δ-Ava-OH was dissolved in 10 mL of DMF in an ice–water bath. H-Phe-OMe was isolated from 8.63 g (40 mmol) of the corresponding methyl ester hydrochloride by neutralization, subsequent extraction with ethyl acetate, and ethyl acetate extract was concentrated to 10 mL. It was then added to the reaction mixture, followed immediately by 4.12 g (20 mmol) of dicyclohexylcarbodiimide (DCC) and 2.7 g (20 mmol) of HOBt. The reaction mixture was allowed to come to room temperature and stirred for 3 days. The residue was taken up in ethyl acetate (40 mL) and dicyclohexylurea (DCU) was filtered off. The organic layer was washed with 1 N HCl (3 × 30 mL), brine (1 × 30 mL), 1 M sodium carbonate (3 × 30 mL), and brine (2 × 30 mL); dried over anhydrous sodium sulfate; and evaporated in a vacuum. A white material was obtained.

Yield: 6.35 g (16.8 mmol, 84%).

^{1}H NMR (300 MHz, $CDCl_3$): δ 7.17−7.32 (m, 5H, Phe(2) phenyl ring protons); 7.10 (d, J = 7 Hz, 1H, Phe(2) NH); 5.95 (br, 1H, δ-Ava(1) NH); 4.86−4.92 (m, 1H, Phe(2) C^α H); 3.73 (s, 3H -OCH_3); 3.03−3.20 (m, 4H, δ-Ava(1) C^δ Hs and Phe(2) C^β Hs); 2.19 (t, J = 7 Hz, 2H, δ-Ava(1) C^α Hs); 1.57−1.67 (m, 4H, δ-Ava(1) C^β Hs and C^γ Hs); 1.44 (s, 9H, Boc CH_3).

(8) (a) Parthasarathy, R.; Chaturvedi, S.; Go, K. *Proc. Natl. Acad. Sci. U.S.A.* **1990**, *87*, 871–875. (b) Guha, S.; Drew, M. G. B.; Banerjee, A. *Tettrahedron Lett.* **2006**, *47*, 7951–7955.

(9) (a) Pan, Y.; Birkedal, H.; Pattison, P.; Brown, D.; Chapuis, G. *J. Phys. Chem. B* **2004**, *108*, 6458–6466. (b) Birkedal, H.; Schwarzenbach, D.; Pattison, P. *Angew. Chem., Int. Ed.* **2002**, *41*, 754–756.

HRMS *m/z* 379.0968 $[M + H]^+$, 401.0699 $[M + Na]^+$, 417.0407 $[M + K]^+$; $M_{calcd} = 378.4614$.

Anal. Calcd for $C_{20}H_{30}N_2O_5$ (378): C, 63.47; H, 7.99; N, 7.40.

Found: C, 63.45; H, 8.02; N, 7.42.

(e) Boc-β-Ala(1)-Ala(2)-OH. To 4.11 g (15 mmol) of Boc-β-Ala(1)-Ala(2)-OMe were added 35 mL of MeOH and 25 mL of 2 N NaOH, and the progress of saponification was monitored by thin-layer chromatography (TLC). The reaction mixture was stirred. After 10 h, methanol was removed under a vacuum, the residue was taken in 50 mL of water, washed with diethyl ether (2 × 50 mL). Then the pH of the aqueous layer was adjusted to 2 using 1 N HCl, and it was extracted with ethyl acetate (3 × 50 mL). The extracts were pooled, dried over anhydrous sodium sulfate, and evaporated in a vacuum. A white crystalline material was obtained.

Yield: 3.43 g (13.2 mmol, 88%).

^{1}H NMR (300 MHz, DMSO-d_6): δ 12.49 (br, 1H, -COOH); 8.16 (d, $J = 7$ Hz, 1H, Ala(2) NH); 6.70 (br, 1H, β-Ala(1) NH); 4.13−4.22 (m, 1H, Ala(2) C^α H); 3.07−3.14 (m, 2H, β-Ala(1) C^β Hs); 2.25 (t, $J = 7$, 2H, β-Ala(1) C^α Hs); 1.37 (s, 9H, Boc CH_3); 1.24 (d, $J = 7$ Hz, 3H, Ala(2) C^β H).

HRMS *m/z* 283.0213 $[M + Na]^+$; $M_{calcd} = 260.2861$.

Anal. Calcd for $C_{11}H_{20}N_2O_5$ (260): C, 50.76; H, 7.74; N, 10.76.

Found: C, 50.79; H, 7.69; N, 10.80.

(f) Boc-δ-Ava(1)-Phe(2)-OH. To 5.67 g (15 mmol) of Boc-δ-Ava(1)-Phe(2)-OMe were added 35 mL of MeOH and 25 mL of 2 N NaOH, and the progress of saponification was monitored by thin-layer chromatography (TLC). The reaction mixture was stirred. After 10 h, methanol was removed under a vacuum and the residue was taken in 50 mL of water and washed with diethyl ether (2 × 50 mL). The pH of the aqueous layer was then adjusted to 2 using 1 N HCl; the aqueous layer was extracted with ethyl acetate (3 × 50 mL). The extracts were pooled, dried over anhydrous sodium sulfate, and evaporated in a vacuum. A white crystalline material was obtained.

Yield: 4.69 g (12.9 mmol, 86%).

^{1}H NMR (300 MHz, DMSO-d_6): δ 12.45 (br, 1H, -COOH); 8.03 (d, $J = 7$ Hz, 1H, Phe(2) NH); 7.12−7.22 (m, 5H, Phe(2) phenyl ring protons); 6.63 (br, 1H, δ-Ava(1) NH); 4.32−4.39 (m, 1H, Phe(2) C^α H); 2.95−3.01 (m, 2H, δ-Ava(1) C^δ Hs); 2.73−2.80 (m, 2H, Phe(2) C^β Hs); 1.92−1.99 (m, 2H, δ-Ava(1) C^α Hs); 1.30 (s, 9H, Boc CH_3); 1.08−1.19 (m, 4H, δ-Ava(1) C^β Hs and C^γ Hs).

HRMS *m/z* 387.0062 $[M + Na]^+$; $M_{calcd} = 364.4349$.

Anal. Calcd for $C_{19}H_{28}N_2O_5$ (364): C, 62.62; H, 7.74; N, 7.69.

Found: C, 62.64; H, 7.71; N, 7.65.

(g) H_3N^+-β-Ala(1)-Ala(2)-COO^- (Peptide **1***).* To 2.60 g (10 mmol) of Boc-β-Ala(1)-Ala(2)-OH was added 4 mL of 98% formic acid, and the removal of the Boc group was monitored by TLC. After 8 h, formic acid was removed under a vacuum. The residue was taken in water (20 mL) and washed with diethyl ether (2 × 30 mL). The pH of the aqueous solution was then adjusted to 8 with 30% aqueous NH_3. The aqueous portion was evaporated in a vacuum to yield peptide **1** as white solid.

Yield: 1.15 g (7.2 mmol, 72%).

mp 220 °C.

$[\alpha]^{20}_D = -22.9$ ($c = 0.2$ in H_2O).

^{1}H NMR [600 MHz, 10% D_2O(v/v)]: δ 8.33 (br, 3H, β-Ala(1) NH_3^+); 8.01 (br, 1H, Ala(2) NH); 3.99−4.04 (m, 1H, Ala(2) C^α H); 3.12−3.19 (m, 2H, β-Ala(1) C^β Hs); 2.57 (t, $J = 6$ Hz, 2H, β-Ala(1) C^α Hs); 1.23 (d, $J = 7$ Hz, 3H, Ala(2) C^β H).

^{1}H NMR (300 MHz, D_2O): δ 4.05 (q, $J = 7$ Hz, 1H, Ala(2) C^α H); 3.19 (t, $J = 6$ Hz, 2H, β-Ala(1) C^β Hs); 2.61 (t, $J = 6$ Hz, 2H, β-Ala(1) C^α Hs); 1.25 (d, $J = 7$ Hz, 3H, Ala(2) C^β H).

^{13}C NMR (75 MHz, D_2O): δ 180.654 (C of COO^-), 171.788 (C of CONH), 51.408 (α-C of Ala), 36.102 (α-C of β-Ala), 32.294 (β-C of β-Ala), 17.405 (β-C of Ala).

DEPT 135 (D_2O): δ 180.654 and 171.788 (disappear); 51.408 and 17.405 (positive); 36.102 and 32.294 (negative).

HRMS *m/z* 161.0866 $[M + H]^+$, 183.0645 $[M + Na]^+$; $M_{calcd} = 160.1706$.

Anal. Calcd for $C_6H_{12}N_2O_3.H_2O$ (178): C, 40.44; H, 7.92; N, 15.72.

Found: C, 40.39; H, 7.88; N, 15.76.

(h) H_3N^+-δ-Ava(1)-Phe(2)-COO^- (Peptide **2***).* To 3.64 g (10 mmol) of Boc-δ-Ala(1)-Phe(2)-OH was added 4 mL of 98% formic acid, and the removal of the Boc group was monitored by TLC. After 8 h, formic acid was removed under a vacuum. The residue was taken in water (20 mL) and washed with diethyl ether (2 × 30 mL). The pH of the aqueous solution was then adjusted to 8 with 30% aqueous NH_3. The aqueous portion was evaporated in a vacuum to yield peptide **2** as white solid.

Yield: 1.95 g (7.4 mmol, 74%).

mp 190 °C.

$[\alpha]^{20}_D = +17.9$ ($c = 0.2$ in H_2O).

^{1}H NMR [600 MHz, 10% D_2O(v/v)] δ 8.32 (br, 3H, δ-Ava(1) NH_3^+); 7.71 (br, 1H, Phe(2) NH); 7.15−7.25 (m, 5H, Phe(2) phenyl ring protons); 4.35−4.38 (m, 1H, Phe(2) C^α H); 3.12 (d, $J = 5$ Hz, 1H, Phe(2) diastereotopic C^β H); 3.09 (d, $J = 5$ Hz, 1H, Phe(2) diastereotopic C^β H); 2.73−2.79 (m, 2H, δ-Ava(1) C^δ Hs); 2.04−2.13 (m, 2H, δ-Ava(1) C^α Hs); 1.20−1.42 (m, 4H, δ-Ava(1) C^β Hs and C^γ Hs).

^{1}H NMR (300 MHz, D_2O) δ 7.17−7.29 (m, 5H, Phe(2) phenyl ring protons); 4.36−4.41 (dd, $J = 5$ Hz, 1H, Phe(2) C^α H); 3.14 (d, $J = 5$ Hz, 1H, Phe(2) diastereotopic C^β H); 3.10 (d, $J = 5$ Hz, 1H, Phe(2) diastereotopic C^β H); 2.75−2.82 (m, 2H, δ-Ava(1) C^δ Hs); 2.09−2.13 (m, 2H, δ-Ava(1) C^α Hs); 1.31−1.44 (m, 4H, δ-Ava(1) C^β Hs and C^γ Hs).

^{13}C NMR (75 MHz, D_2O): δ 178.188 (C of COO^-), 175.103 (C of CONH), 137.888 (one phenyl ring C attached with CH_2), 129.235 (m-C's of phenyl ring), 128.569 (o-C's of phenyl ring), 126.732 (p-C of phenyl ring), 56.225 (α-C of Phe), 38.984 (δ-C of δ-Ava), 37.727 (β-C of Phe), 34.808 (α-C of δ-Ava), 25.941 (γ-C of δ-Ava), 21.990 (β-C of δ-Ava).

DEPT 135 (D_2O): δ 178.188, 175.103, and 137.888 (disappear); 129.235, 128.569, 126.732, and 56.225 (positive); 38.984, 37.727, 34.808, 25.941 and 21.990 (negative).

HRMS *m/z* 265.1355 $[M + H]^+$, 287.1206 $[M + Na]^+$; $M_{calcd} = 264.3194$.

Anal. Calcd for $2(C_{14}H_{20}N_2O_3).2H_2O$ (564): C, 59.56; H, 7.85; N, 9.92.

Found: C, 59.61; H, 7.82; N, 9.87.

NMR Experiments. All 300 MHz NMR studies were carried out on a Brüker DPX 300 MHz spectrometer at 300 K and 600 MHz NMR studies were carried out on a Brüker AVANCE 600 MHz spectrometer at 278 K using cryo probe.

FT-IR Spectrometer. Spectra were collected on a JASCO instrument, Model FT/IR-4200 typeA. For the solution state, CaF_2 cell was used. Concentration 3 mg mL^{-1}.

Mass Spectrometry. Mass spectra were recorded on a Qtof Micro YA263 high-resolution mass spectrometer.

Polarimeter. PerkinElmer instrument. Model 341 LC Polarimeter.

Transmission Electron Microscopy. Transmission electron microscopy (TEM) was carried out to investigate the morphology of the nanostructures. TEM images were recorded on a FEI (Tecnai spirit) instrument. Images were taken at 80 KV.

CD Spectrometer. All spectra were recorded on a JASCO instrument, Model J-815–150S. For temperature dependent experi-

ment we use Peltier-type thermostat and purged continuously with dry N_2 gas at 15 L min^{-1} during data acquisition. Data were collected in a quartz cuvette with a path length of 1 mm between 190 and 250 nm.

X-Ray Powder Diffraction. Temperature-dependent XRPD (room temperature and 50−100 °C) were recorded on a X Pert PRO high-resolution X-ray diffractometer instrument.

Results and Discussion

Single Crystal X-Ray Diffraction Study. Two water soluble dipeptides, where ω-amino acid is used in the N-terminus, β-Ala-L-Ala (**1**) and δ-Ava-L-Phe (**2**), have been synthesized by conventional solution-phase methodology,[10] purified, characterized, and studied. Colorless triclinic crystals of peptide **1** and colorless monoclinic crystals of peptide **2**, suitable for X-ray diffraction studies, were obtained from their aqueous solutions by slow evaporation.[11] Peptide **1** crystallizes with one peptide molecule and one water molecule in the asymmetric unit and peptide **2** crystallizes with two peptide molecules and two water molecules in the asymmetric unit (Figure 1). In both cases, N-terminally located β-Ala and δ-Ava residues adopt an extended backbone conformation around the −C−C− bond(s) of the oligomethylene units (Tables 1 and 2). Water molecules play an important role in the formation and stabilization of hydrogen-bonded nanotubular structure along the crystallographic *b* axis (panels a and b in Figure 2). For peptide **1**, $NH_3^+\cdots{}^-OOC$ (head to tail), $NH_3^+\cdots O(W)$, $H(W)\cdots{}^-OOC$, $NH_3^+\cdots O{=}C$ (amide), and amide $NH\cdots{}^-OOC$ intermolecular hydrogen bonds are involved in the formation of nanotubular architecture (Table 3). For peptide **2**, $NH_3^+\cdots{}^-OOC$ (head to tail), $NH_3^+\cdots O(W)$, $H(W)\cdots{}^-OOC$, $H(W)\cdots O{=}C$ (amide), and amide $NH\cdots O{=}C$ (amide) intermolecular hydrogen bonds are involved in the formation of nanotubar architecture (Table 4). The DPNT **2** is further stabilized by aromatic π−π stacking with average π−π distance of 4.9 Å (centroid-centroid distance). Peptides **1** and **2** form hydrogen-bonded water-mediated DPNTs with approximate dimensions of 2.8 Å × 5.8 Å and 3.0 Å × 6.5 Å, respectively, in the solid state and the channels are essentially chiral due to the presence of C-terminally located chiral amino acid (Ala/Phe) residues.

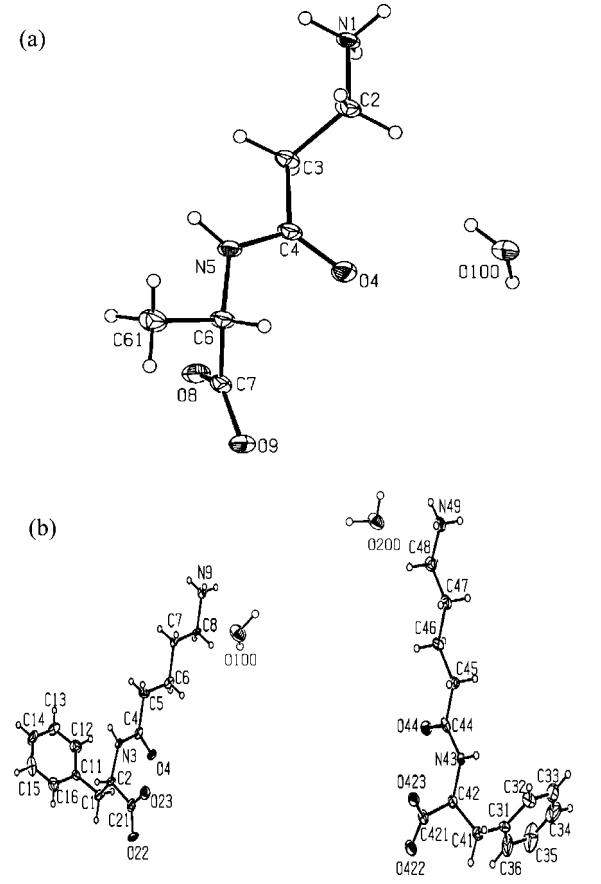

Figure 1. (a, b) ORTEP diagrams with atomic numbering scheme of peptides **1** and **2**, respectively. Thermal ellipsoids are at the 30% probability level. Peptide **1** crystallizes with one peptide molecule and one water molecule in the asymmetric unit. Peptide **2** crystallizes with two peptide molecules and two water molecules in the asymmetric unit.

Table 1. Selected Backbone Torsional Angles (deg) of Dipeptide 1

torsion angles	values (deg)
N1−C2−C3−C4 (θ1)	−174.8(2)
C2−C3−C4−N5 (ψ1)	−121.0(3)
C3−C4−N5−C6 (ω1)	−174.7(2)
C4−N5−C6−C7 (φ2)	64.9(3)
N5−C6−C7−O8	28.7(3)
N5−C6−C7−O9	−153.7(2)

Thermogravimetric Analysis (TGA) and Differential Thermal Analysis (DTA) Experiments. DPNTs **1** and **2** showed significant thermal stability in the solid state, as demonstrated by TGA-DTA (TGA, thermogravimetric analysis; DTA, differential thermal analysis) experiments. The TGA experiments showed that water molecules are removed with a weight loss of 10.03% and 6.18% in the temperature range 25−100 °C for peptides **1** and **2** respectively that compares well with the theoretical value of 10.11% for the loss of one water molecule for peptide **1** and 6.38% for the loss of two water molecules for peptide **2**. Decomposition of peptides **1** and **2** begins at ∼220 °C and ∼190 °C respectively. The DTA plots show one endotherm centered at ∼80 °C due to the loss of one water molecule for peptide

(10) Bodanszky, M.; Bodanszky, A. *The Practice of Peptide Synthesis*; Springer-Verlag: New York, 1984; pp 1–282..
(11) Crystal data for peptide **1**: $C_6H_{12}N_2O_3$, H_2O, M_r = 178.19, crystal dimensions 0.30 × 0.05 × 0.05 mm^3, triclinic, space group $P\bar{1}$, a = 5.7442 (17) Å, b = 8.994 (3) Å, c = 9.140 (3) Å, α = 97.33 (3)°, β = 100.98 (3)°, γ = 102.89 (2)°, V = 444.7 (2) $Å^3$, Z = 2, ρ_{calcd} = 1.331 g cm^{-3}, μ = 0.111 (mm^{-1}), $2\theta_{max}$ = 60.0°. Crystal data for peptide **2**: $2(C_{14}H_{20}N_2O_3)$, $2H_2O$, M_r = 564.67, crystal dimensions 0.30 × 0.05 × 0.05 mm^3, monoclinic, space group $P2_1$, a = 4.8848 (11) Å, b = 28.461 (7) Å, c = 10.9493 (15) Å, β = 102.655 (16)°, V = 1485.2 (5) $Å^3$, Z = 2, ρ_{calcd} = 1.263 g cm^{-3}, μ = 0.093 (mm^{-1}), $2\theta_{max}$ = 60.0°. Diffraction data were measured with Mo K_α (λ = 0.71073 Å) radiation at 150 K using an Oxford Diffraction X-Calibur CCD system. Data analyses were carried out with the Crysalis program.[12] The structures were solved by direct methods using the SHELXS-97[13] program. Refinements were carried out with a full matrix least squares method against F^2 using SHELXL-97.[14] The non-hydrogen atoms were refined with anisotropic thermal parameters. The hydrogen atoms were included in geometric positions and given thermal parameters equivalent to 1.2 times those of the atom to which they were attached. The final R-values were R1 = 0.0690, 0.0757 and wR2 = 0.1827, 0.1694 for 1255, 1585 data with $I > 2\sigma(I)$ for peptides **1** and **2**, respectively. Crystallographic data have been deposited at the Cambridge Crystallographic Data Centre with reference numbers CCDC 648388 and 648389.
(12) *Crysalis*, version 1.0; Oxford Diffraction: Oxfordshire, U.K., 2006.
(13) Sheldrick, G. M. *Acta Crystallogr., Sect. A* **1990**, *46*, 467–473.
(14) Sheldrick, G. M. *SHELX-97, Program for Crystallography Refinement*; University of Göttingen: Göttingen, Germany, 1997.

Table 2. Selected Backbone Torsional Angles (deg) of Dipeptide 2

molecule 1		molecule 2	
torsion angles	values (deg)	torsion angles	values (deg)
N9−C8−C7−C6 ($\theta_1$1)	−178.5(4)	N49−C48−C47−C46 ($\theta_1$1)	−176.5(5)
C8−C7−C6−C5 ($\theta_2$1)	−169.1(5)	C48−C47−C46−C45 ($\theta_2$1)	179.6(5)
C7−C6−C5−C4 ($\theta_3$1)	−177.9(5)	C47−C46−C45−C44 ($\theta_3$1)	177.3(6)
C6−C5−C4−N3 (ψ1)	168.2(5)	C46−C45−C44−N43 (ψ1)	175.2(6)
C5−C4−N3−C2 (ω1)	179.7(5)	C45−C44−N43−C42 (ω1)	172.6(5)
C4−N3−C2−C21 (φ2)	59.0(7)	C44−N43−C42−C421 (φ2)	−72.1(7)
N3−C2−C21−O22	−144.8(5)	N43−C42−C421−O422	160.8(5)
N3−C2−C21−O23	36.8(8)	N43−C42−C421−O423	−18.7(8)

1 and one endotherm also centered at ∼80 °C due to the loss of two water molecules for peptide **2**. The TGA-DTA experiments were also performed for peptides **1** and **2** (crystals) that were heated at about 100 °C under vacuum (0.1 mm) for 2 h and showed that no water molecules are present in the crystal lattice. TGA-DTA studies of the re-exposed dehydrated crystals of these dipeptides to water vapor for 2 days revealed that loss of water molecules occur in a reversible manner (see the Supporting Information, Figures S1 and S2).

X-Ray Powder Diffraction (XRPD) Studies. The crystals of peptides **1** and **2** were grounded to a powder and examined by X-ray powder diffraction (XRPD). The simulated XRPD patterns from single-crystal data of peptides **1** and **2** closely match with the experimentally observed patterns, supporting the hypothesis that the bulk powder retains a structural similarity to the single crystal. In order to examine the thermal stability of these nanotubes and the role of water molecules in the nanotube formation in the solid state, we have performed temperature dependent (50−100 °C) XRPD experiments. From temperature dependent XRPD experiments, it is clear that up to 70 °C diffraction patterns and intensities remain unchanged for both peptides **1** and **2**. The XRPD patterns of peptide **1** at 80 °C and above show that peaks at 2θ = 9.514° (h = 0, k = 1, l = 0), 11.182° (01−1), 13.907° (011), 17.561° (002) remain unaltered, and the intensity of the peak at 2θ = 19.115° (01−2) increases. The XRPD patterns of peptide **2** at 80 °C and above show that peaks at 2θ = 10.317° (021), 12.419° (040), 16.843° (012), 18.677° (060), and 22.073° (11−2) remain unaltered, the intensity of the peak at 2θ = 8.823° (011) decreases, and the intensity of the peak at 2θ = 20.530° (061) increases. These differences in the diffraction intensities of the dehydrated peptides **1** and **2** indicate that structural deformation occurs when the water molecules are removed (80 °C) from the crystal lattice. For the dehydrated peptides **1** and **2**, simulated XRPD patterns were calculated simply by omitting the water molecules from the single-crystal X-ray structure. XRPD analyses of the re-exposed dehydrated crystals of these dipeptides to water vapor for 2 days revealed that loss of water molecules occur in a reversible manner (panels a and b in Figure 3). We were unable to obtain crystals of the dehydrated material, which confirms the importance of the water molecules to the efficient packing of these peptides.

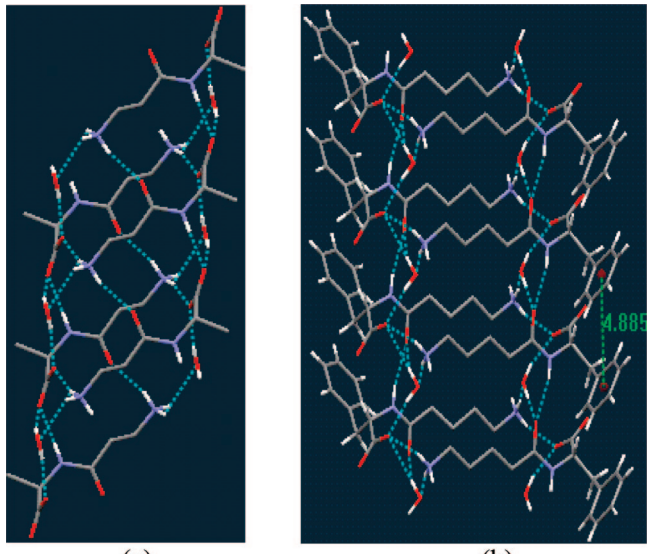

Figure 2. (a, b) Formation of hydrogen-bonded water-mediated nanotubular architectures of dipeptides **1** and **2**, respectively, along the crystallographic *b*-axis.

Table 3. Hydrogen Bond Parameters of Dipeptide 1[a]

D−H···A	H···A (Å)	D···A (Å)	D−H···A (deg)
O100−H1···O9 (a)	1.98(3)	2.770(3)	163(3)
N1−H1A···O100 (b)	1.87	2.753(3)	173
N1−H1B···O8 (c)	1.90	2.754(3)	161
N1−H1C···O4 (a)	1.95	2.824(3)	165
O100−H2···O8	1.90(4)	2.730(3)	168(3)
N5–H5···O9 (a)	2.00	2.826(3)	160

[a] Symmetry elements: (a) −1 + x, y, z; (b) x, 1 + y, z; (c) 1 − x, 1 − y, 2 − z.

Transmission Electron Microscopic (TEM) Studies. Transmission electron microscopic (TEM) studies of peptides **1** and **2** were carried out using an aqueous solution of the corresponding compounds (3 mg mL^{-1}) on a carbon coated copper grid (300 mesh) by slow

Table 4. Hydrogen Bond Parameters of Dipeptide 2[a]

D−H···A	H···A (Å)	D···A (Å)	D−H···A (deg)
N3−H3···O4 (a)	2.14	2.958(6)	157
N9−H9A···O23 (b)	2.29	2.989(6)	135
N9−H9A···O423 (c)	2.54	3.099(6)	122
N9−H9B···O100	1.90	2.770(6)	166
N9−H9C···O22 (d)	1.84	2.729(6)	175
N43−H43···O44 (a)	2.14	2.950(6)	156
N49–H49A···O423 (b)	2.19	2.917(6)	139
N49−H49A···O23 (e)	2.59	3.082(6)	116
N49−H49B···O422 (d)	1.85	2.729(6)	170
N49−H49C···O200	1.92	2.802(6)	170
O100−H102···O44 (c)	1.98(4)	2.815(6)	165(5)
O100−H101···O423 (f)	1.87(5)	2.686(5)	163(4)
O200−H201···O4 (e)	2.11(5)	2.828(6)	133(4)
O200−H202···O23 (f)	1.87(5)	2.741(6)	169(4)

[a] Symmetry elements: (a) 1 + x, y, z; (b) x, y, 1 + z; (c)1 − x, −0.5 + y, 2 − z; (d) 1 + x, y, 1 + z; (e) 1 − x, 0.5 + y, 2 – z; (f) 2 – x, 0.5 + y, 2 − z.

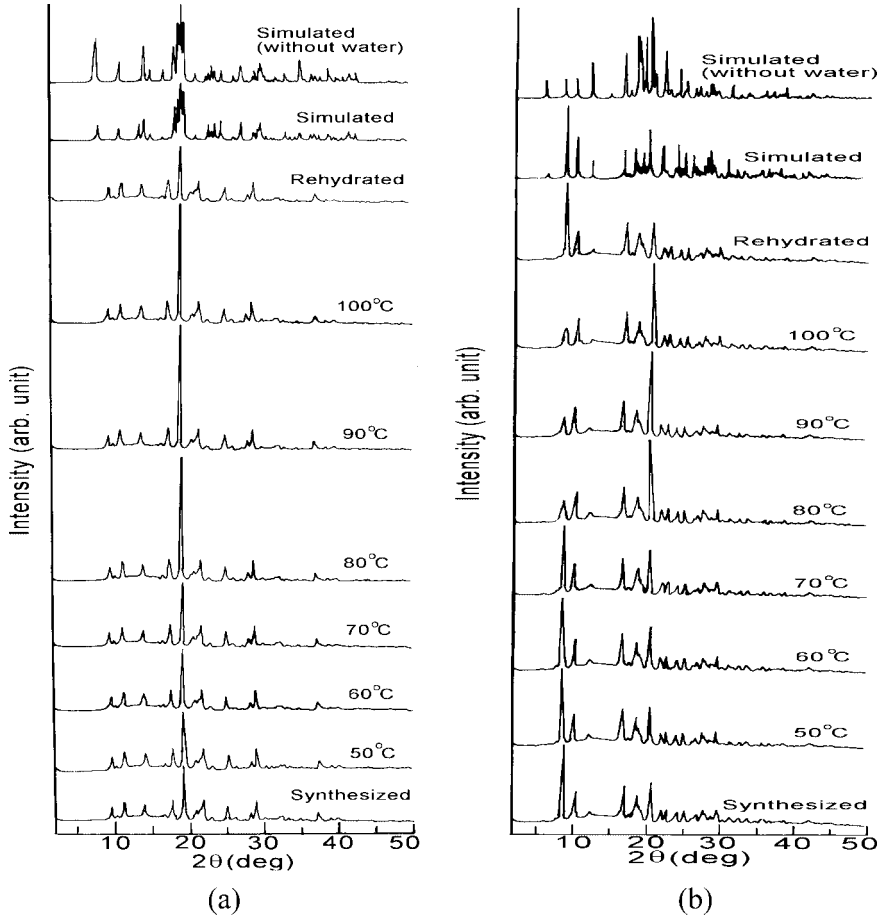

Figure 3. (a, b) XRPD patterns of dipeptides **1** and **2**, respectively, as-synthesized (grounded crystals at room temperature), at different temperatures (50 °C−100 °C), re-exposed dehydrated crystals to water vapor for 2 days, simulated from single-crystal data, and simulated simply by omitting the water molecules from the single-crystal X-ray structures.

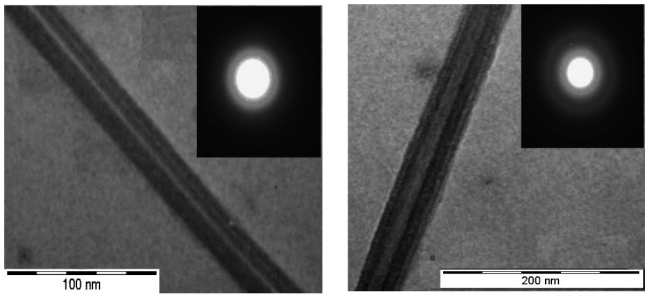

Figure 4. (a, b) TEM images of hollow nanotubular structures formed by peptides **1** and **2**, respectively. Electron Diffraction patterns of DPNTs **1** and **2** are shown in the insets of the respective figures.

evaporation and vacuum drying at 30 °C for 2 days. The TEM image of the dipeptide **1** shows a uniform and well-ordered hollow nanotube of 27 nm total diameter with a 5 nm inner diameter and the TEM image of the dipeptide **2** also shows a uniform and well-ordered hollow nanotube of 44 nm total diameter with a 15 nm inner diameter and no amorphous aggregation was observed (Figure 4). The morphological feature of the dipeptides **1** and **2** were investigated under a broad range of pH and the morphology of the nanotubular structures remained unchanged over these wide ranges of pH (Figure 5a−d). We use ω-amino acid in the N-terminus instead of previously reported α-amino acid to incorporate a proteolytically stable C−C bond into the peptide backbone. We observed that the nanotubular structures remained unaltered in morphology after the incubation of these peptides with Proteinase K (0.02 mg mL^{-1}) for more than 24 h (images e and f in Figure 5). This indicates the enzymatic stability of this new class of DPNTs against protease degradation. To examine the thermal stability of these nanotubes, TEM grids were prepared from the hot (80 °C) aqueous solutions of peptides **1** and **2** and TEM experiments were done by the usual procedure. It has been observed that these nanotubes are also stable at a high temperature (80 °C) in aqueous solutions (images g and h in Figure 5).

Circular Dichroic (CD) and Fourier Transformed Infrared (FT-IR) Spectroscopic Studies. We have performed the circular dichroic (CD) and Fourier transformed infrared spectroscopic (FTIR) experiments of peptides **1** and **2** in aqueous solution to examine their secondary structural informations. The CD spectra of peptides **1** and **2** are different. Peptide **1** shows a strong negative band at 203 nm ($\pi-\pi^*$ transition) and a weak positive band at 233 nm ($n-\pi^*$ transition), whereas the peptide **2** shows a strong positive band at 196 nm ($\pi-\pi^*$ transition) and a second positive band near 214 nm ($n-\pi^*$ transition). Incorporation of oligomethylene units ($-(CH_2)_2-$ unit for β-Ala residue and $-(CH_2)_4-$ unit for δ-Ava residue) in place of an amide bond is expected to perturb the observed CD-spectrum.[15] We have performed variable temperature (20−80 °C) CD experiments[6a] to

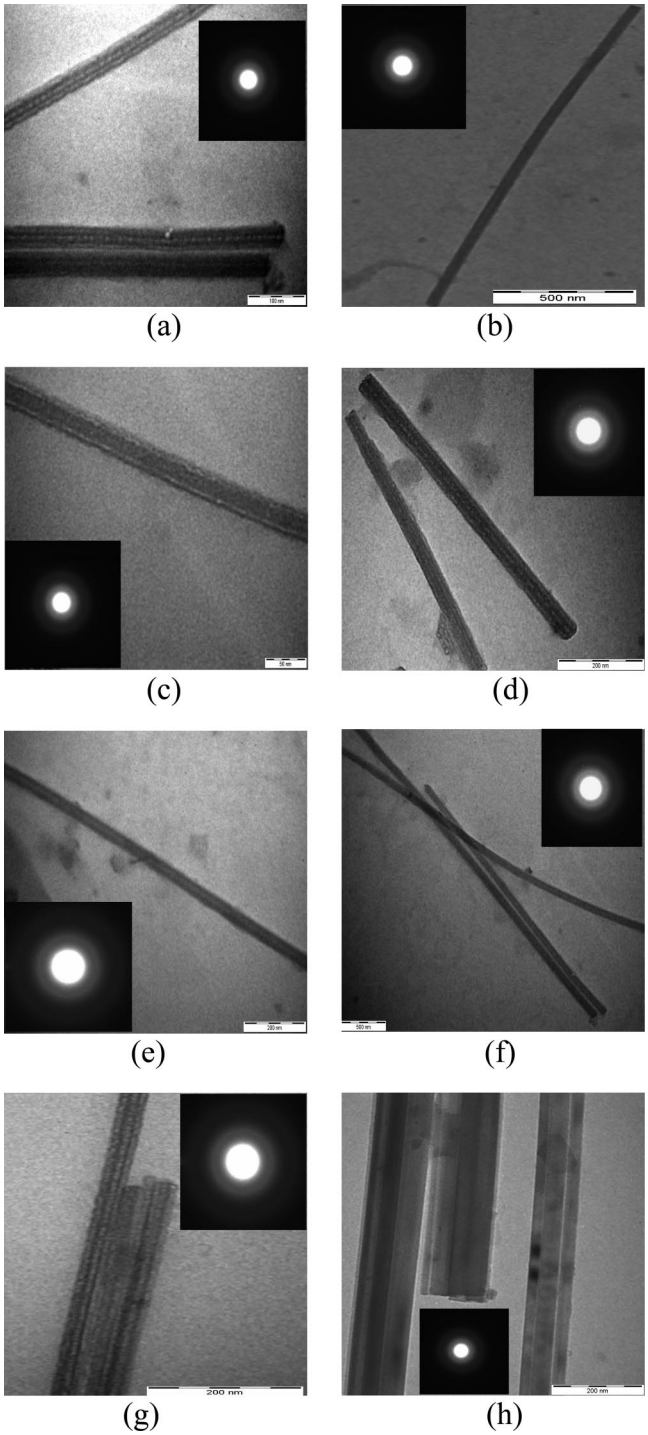

Figure 5. TEM images demonstrating the stability of DPNTs **1** and **2**, respectively, under different pH conditions: (a, b) acidic (pH 1); (c, d) alkaline (pH 13); (e, f) after 24 h Proteinase K treatment in 50 mM tris-HCl at pH 7.2; (g, h) after heating the aqueous solutions at 80 °C.

monitor the thermal stability of these DPNTs in solution, and it has been found that no significant structural deformation occurs up to a high temperature (80 °C) indicating their thermal stability in aqueous solution (Figure 6).

FT-IR spectra of peptide **1** in D_2O (after D_2O subtraction) showed a sharp peak at 1638.02 cm^{-1} at the amide I region (amide CO stretching), and 1565.05 cm^{-1} at amide II region

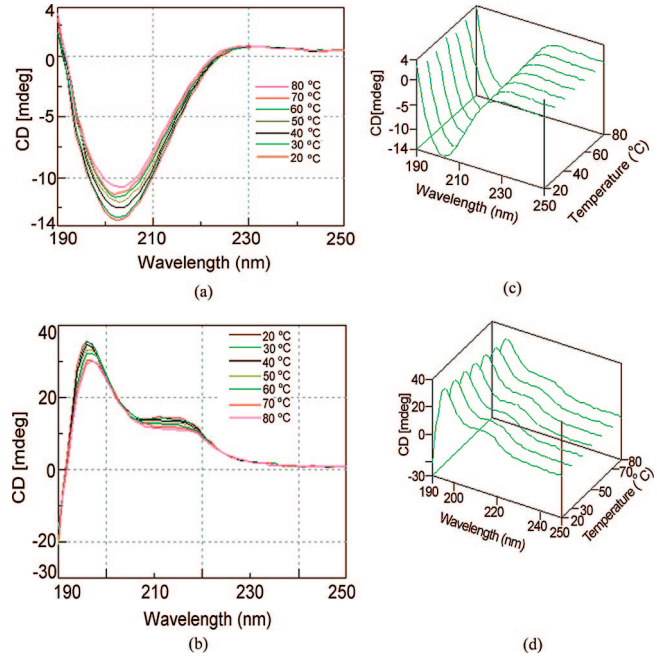

Figure 6. (a, b) Variable-temperature CD spectra of peptides **1** and **2**, respectively, showing significant thermal stability (20−80 °C) in aqueous solution. (c, d) 3D variable temperature CD curves of peptides **1** and **2**, respectively.

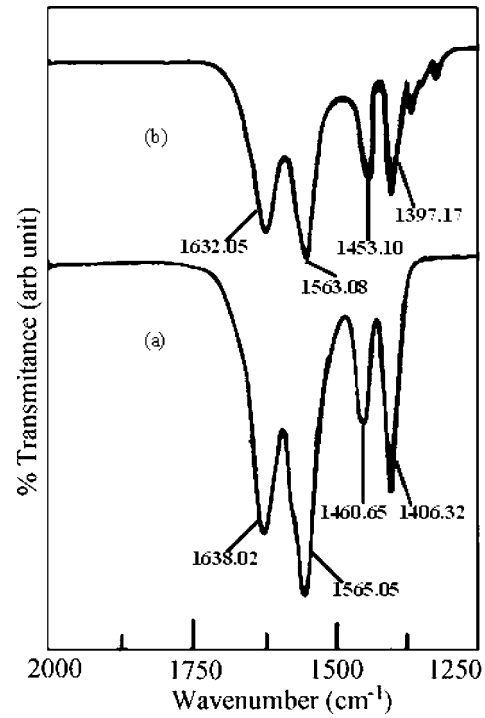

Figure 7. (a, b) FT-IR spectra of peptides **1** and **2**, respectively, in D_2O.

(NH bending) (Figure 7a). FT-IR data of peptide **1** are closely related to a β-sheet-like conformation in solution.[16] Peptide **2** showed (after D_2O subtraction) a sharp peak at 1632.05 cm^{-1} at the amide I region (amide CO stretching), and

(15) Banerjee, A.; Pramanik, A.; Bhattachariya, S.; Balaram, P. *Biopolymers* **1996**, *39*, 769–777.

(16) (a) Moretto, V.; Crisma, M.; Bonora, G. M.; Toniolo, C.; Balaram, H.; Balaram, P. *Macromolecules* **1989**, *22*, 2939–2944. (b) Zandomeneghi, G.; Krebs, M. R. H.; Mccammon, M. G.; Fandrich, M. *Protein Sci.* **2004**, *13*, 3314–3321. (c) Mazor, Y.; Gilead, S.; Benhar, I.; Gazit, E. *J. Mol. Biol.* **2002**, *322*, 1013–1024.

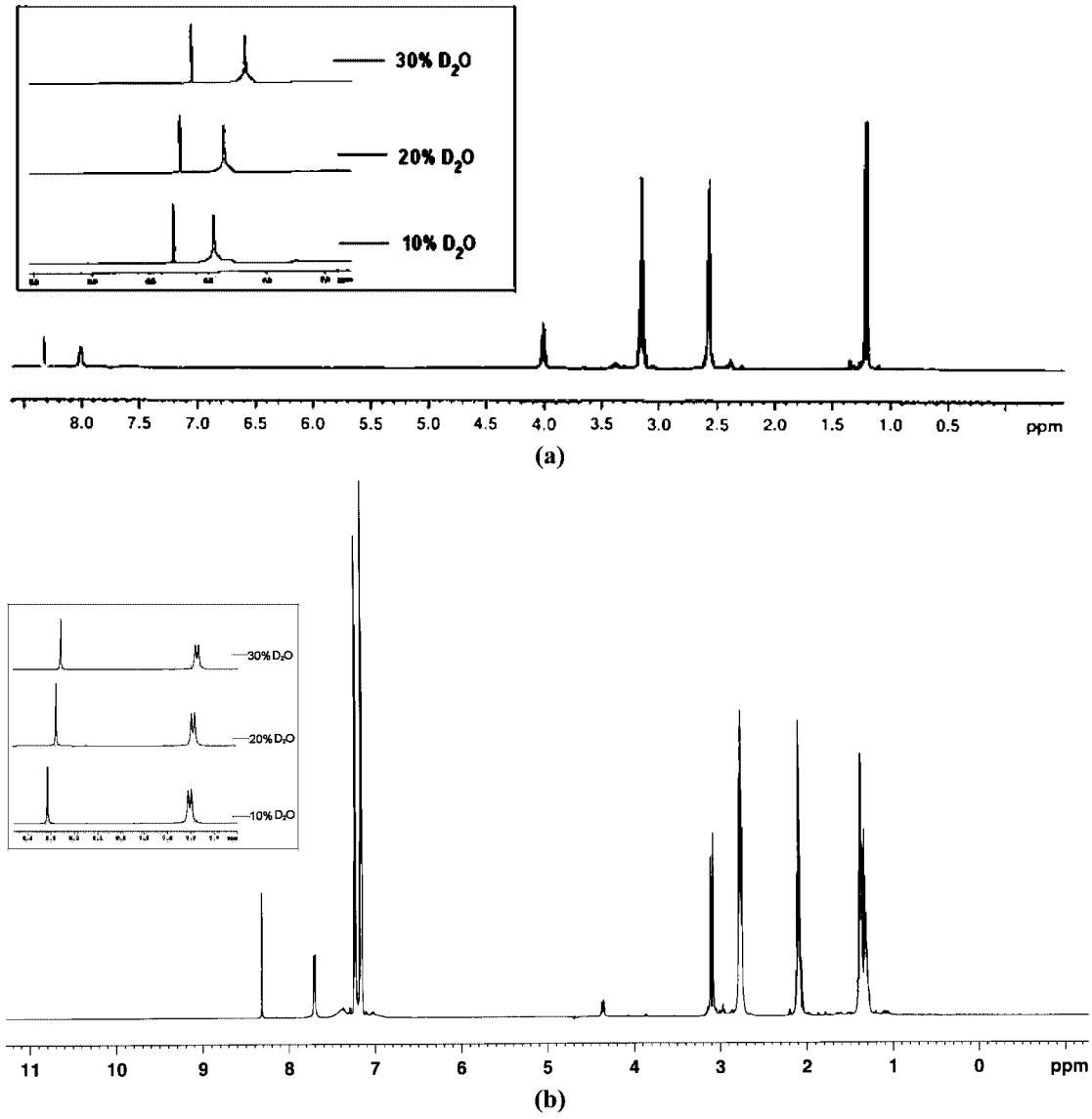

Figure 8. (a, b) ^{1}H NMR spectra of peptides **1** and **2**, respectively, in 10% D_2O (v/v). It is interesting to note that NH_3^+ and amide NH of peptides **1** and **2** are not exchanged in 10, 20, and in 30% D_2O, which are also shown in the inset of the respective figures.

1563.08 cm^{-1} at amide II region (NH bending) (Figure 7b). FT-IR data of peptide **2** are also consistent with a β-sheet conformation in solution.[1a,16]

Solution-State ^{1}H NMR Study. Conformationally restricted nonprotein amino acids, such as, α-amino isobutyric acid (Aib), dehydro phenylalanine (Δ-Phe) are generally used to impose stereochemical restrictions on peptide backbone and thereby dictate peptide chain folding and they are used as models for β-turn structure.[17,1d] However, each of the reported dipeptides **1** and **2** contains a flexible ω-amino acid resudue (β-Ala/δ-Ava) at the N-terminal position, which lacks a side chain and thus, these flexible ω-amino acids possess much more conformational freedom than Aib or Δ-Phe. To investigate their structures in solution state, hydrogen–deuterium (NH/ND) exchange studies[18] have been done using 600 MHz ^{1}H NMR at 25 °C in increasing amount of D_2O in aqueous solutions of peptides **1** and **2** (10% D_2O(v/v), 20% D_2O(v/v), and in 30% D_2O(v/v)) at different time intervals (2 min, 1 h, 12 h, 10 days). The required percentages of D_2O in the aqueous solutions of peptides **1** and **2** have been adjusted after adding appropriate amounts of D_2O to the respective peptide solutions. However, no changes in ^{1}H NMR spectra of the peptides **1** and **2** have been observed even up to 10 days for each D_2O containing samples. It is also interesting to note that NH_3^+ and amide NH are not exchanged in 10, 20, or 30% D_2O even up to 10 days (panels a and b in Figure 8). Only slightly upfield shift of NH_3^+ and amide NH peaks occur when D_2O percentage increases. The upfield shift can occur due to the dilution effect. The more we increase the dilution the more hydrogen-bonded supramolecular aggregation of peptides breaks down causing an upfield shift of the respective NHs which were previously

(17) (a) Aravinda, S.; Shamala, N.; Rajkishore, R.; Gopi, H. N.; Balaram, P. *Angew. Chem., Int. Ed.* **2002**, *41*, 3863–3865. (b) Venkatraman, J.; Shankaramma, S. C.; Balaram, P. *Chem. Rev.* **2001**, *101*, 3131–3152. (c) Banerjee, A.; Datta, S.; Pramanik, A.; Shamala, N.; Balaram, P. *J. Am. Chem. Soc.* **1996**, *118*, 9477–9483. (d) Ramagopal, U. A.; Ramakumar, S.; Sahal, D.; Chauhan, V. S. *Proc. Natl. Acad. Sci. U.S.A.* **2001**, *98*, 870–874.

(18) Polshakov, V. I.; Birdsall, B.; Feeney, J. *J. Mol. Biol.* **2006**, *356*, 886–903.

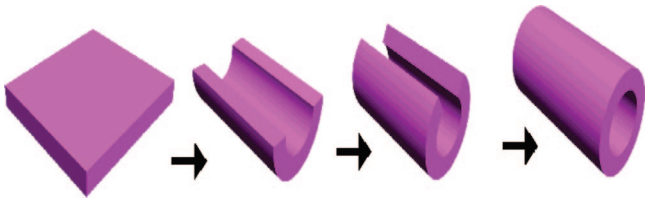

Figure 9. Schematic model of nanotube formation in aqueous solution of peptides **1** and **2**. Peptides **1** and **2** form extended β-sheet structure and closure of the extended sheet along one axis of the two-dimensional layer leads to the formation of the nanotubular structure in solution.

engaged in intermolecular hydrogen bonding. We have increased D_2O percentage in the same NMR tube without adding peptides in D_2O, because we have previously done 300 MHz ^{1}H NMR spectra of peptides **1** and **2** in pure D_2O and we do not get any peak for NH_3^+ and amide NH due to NH/ND exchange (see the Supporting Information, Figures S3 and S4). So, from ^{1}H NMR experiments in 10, 20, and 30% D_2O, it may be concluded that NH_3^+ and amide NH are not solvent-exposed[18] and these NHs are most probably intermolecularly hydrogen-bonded as they are expected to form extended backbone conformation due to the lack of stereochemically constraint amino acid residue in the peptide backbone and this is also in good agreement with X-ray crystal structure. Thus, it can be stated that each molecule is intermolecularly hydrogen-bonded to form self-assembled β-sheet structure, which is also supported by solution-state FT-IR data. The closure of the extended β-sheet structure along one axis of the two-dimensional layer using intermolecular hydrogen bonding and/or aromatic π-π stacking can lead to the formation of the nanotubular structure in solution (Figure 9).[1b,6b,19]

X-Ray Crystal Structure Versus TEM Data. Although these reported dipeptides form nanotubes both in the solid state as well as in solution, their self-assembling pattern in these two states are different. In the solid state, the water molecules play an important role in the formation and stabilization of the hydrogen-bonded nanotubular structures with a small internal diameter (2.8 Å × 5.8 Å for peptide **1** and 3.0 Å × 6.5 Å for peptide **2**). However, in solution-state, internal diameters (5 nm for peptide **1** and 15 nm for peptide **2**) and the total width of these nanotubes are quite large (27 nm for peptide **1** and 44 nm for peptide **2**). From solution state ^{1}H NMR and FT-IR data, it is revealed that peptides **1** and **2** form extended β-sheet structures and these sheet structures may be rolled to form nanotubular structure in solution and an analogy can be drawn with the formation of carbon nanotubes from carbon layerd structure.[19]

(19) Tenne, R. *Angew. Chem., Int. Ed.* **2003**, *42*, 5124–5132.

Conclusions

We present here two unique examples of dipeptide nanotubes, in which water molecules play a vital role in the formation and stabilization of the hydrogen-bonded water-mediated DPNTs in crystals, unlike the previously reported DPNTs[5c–e,9] in which the peptide molecules are self-assembled to form the basic structural unit leaving behind a channel that is filled up by trapped water molecules. These reported dipeptides also form hollow nanotubular structures in aqueous solution. Thermal, proteolytic, and pH stability over a broad range of pH (1−13) can make these nanotubes interesting candidates for future nanotechnological applications.

Acknowledgment. We thank the EPSRC and the University of Reading, U.K., for funds for the Oxford Diffraction X-Calibur CCD-System. S. G. wishes to acknowledge the CSIR, New Delhi, India, for financial assistance. We are thankful to CSIR for funding.

Supporting Information Available: ^{1}H NMR and ^{13}C NMR spectra, and HRMS spectra of the reported dipeptides **1** and **2** (PDF). This information is available free of charge via the Internet at http://pubs.acs.org.

CM703159B